

Shock Tunnel Measurements of Hypervelocity Blunted Cone Drag

L. M. Porter,* A. Paull,† D. J. Mee,‡
and J. M. Simmons§

The University of Queensland,
St. Lucia, Queensland 4072, Australia

Introduction

PRESENTED here are results obtained from an investigation into the effects of nose bluntness on slender cone drag in the hypervelocity flight regime (flight speeds > 5 km/s). Experiments on a 5-deg semi-vertex angle, variable nose tip cone at zero angle of attack were conducted in the T4 free piston driver shock tunnel¹ at a free-stream Mach number of 5.2 and stagnation enthalpy of 14.9 MJ/kg. The drag was measured using the technique developed by Sanderson and Simmons² for use in impulse facilities.

In recent years there has been a renewed interest in the development of hypervelocity vehicles and such propulsion systems as the scramjet engine. Research into the aerodynamic characteristics of the blunted cone with the hypersonic similarity parameter $M_\infty \alpha < 1$, where M_∞ is the free-stream Mach number and α is the cone half-angle in radians, has relevance to the design of scramjet intakes. Research into such cones in subsonic and supersonic flight regimes is extensive, but in the hypervelocity regime this is not the case. A free-flight investigation of the aerodynamics of a blunted 10-deg semi-angle cone has been performed in a hyperballistic range.³

Impulse facilities, such as free piston driver shock tunnels, have been developed to enable investigation into both the hypersonic and hypervelocity regimes. The test time in these facilities is of the order of 1 ms. This short test time prohibits force component measurement with conventional force or accelerometer balances. The stress wave force balance developed by Sanderson and Simmons² relies on interpretation of the transient stress waves propagating within the model and its supporting structure. This approach accounts for the distributed mass effects of the model and force balance structure which are significant in short test times.

Sanderson and Simmons² applied the technique to a 15-deg semi-vertex angle cone which has a uniform surface pressure distribution and a large resulting drag force. Sanderson et al.⁴ extended the technique to application to a longer cone of 5-deg semi-vertex angle. The magnitude of the drag force is smaller on the more slender cone. The work presented here represents a further extension of the technique to measuring the drag due to non-uniform load distributions such as found over blunted bodies.

Experiments

Model

Experiments were performed on a 5-deg semi-vertex angle cone with interchangeable nose tips. The cone had a base radius of 50 mm. Eleven different nose tips were used ranging in radius from 0.2 mm to 18.0 mm in steps of 1.8 mm. These correspond to bluntness ratios ranging from 0.004 to 0.36 in steps of 0.036. The bluntness ratio is defined as the ratio of the nose radius to the cone base radius. The length of the model with the pointed nose tip was 517.5 mm. All experiments were performed with the model aligned axially with the flow.

Drag Measurement Technique

The model is attached to a sting which takes the form of a slender elastic bar (Fig. 1). The sting is suspended by vertical threads to

allow free movement in the axial direction. Strain gauges located on the sting record the passage of stress waves resulting from the rapidly applied aerodynamic loads as they are transmitted from the model into the sting.

Following Sanderson and Simmons² the dynamic behaviour of the model/sting combination may be analytically modelled as a time-invariant, linear system described by the convolution integral,

$$y(t) = \int_0^t g(t - \tau)u(\tau)d\tau \quad (1)$$

where $u(t)$ is the single input to the system, $y(t)$ the resulting output, $g(t)$ the unit impulse response function, t the time, and τ a dummy variable of integration. Knowing the response of the system to a unit impulsive force $g(t)$, it is possible to determine the response of the system $y(t)$ to excitation by any arbitrary force $u(t)$ via Eq. (1). Alternatively, and what is done here, $y(t)$ is obtained from the strain gauge output, and a numerical deconvolution process is performed to obtain $u(t)$, the time history of drag applied to the model.

The unit impulse response function is obtained numerically from a dynamic finite element code. These theoretical results are in good agreement with results obtained experimentally.

Theoretical analysis of a distributed mass model of the model/sting system shows that the mechanical time constant of the force balance is proportional to the mass of the model. A smaller time constant is desirable as it leads to deconvoluted force time histories of greater signal-to-noise ratio. Thus, in order that the mechanical time constant of the system be kept small, the base area of the cone model was hollowed out to reduce the mass of the cone by almost 50%.

Choice of model and sting materials was also dictated by the system time constant. The model was made of aluminium and the sting was made of brass. The sting was 2.3 m long allowing sufficient time for the strain gauge measurements to be made before the return of the stress wave reflected from the free end of the sting. The sting had an outside diameter of 34.9 mm and a wall thickness of 1.6 mm.

Test Flow Conditions

The experiments were performed in the T4 free piston driver shock tunnel facility.¹ A contoured axisymmetric nozzle was used to expand the test gas from the stagnation region to the appropriate test conditions. The nozzle exit plane was 265 mm in diameter and the nozzle throat diameter was 25 mm. The tunnel was operated in a tailored mode so that the mean static pressure and enthalpy were

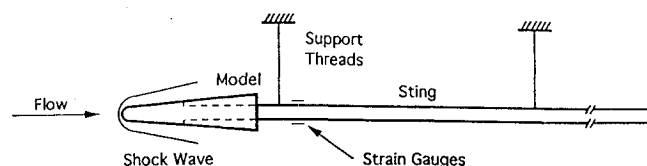


Fig. 1a Force balance configuration.

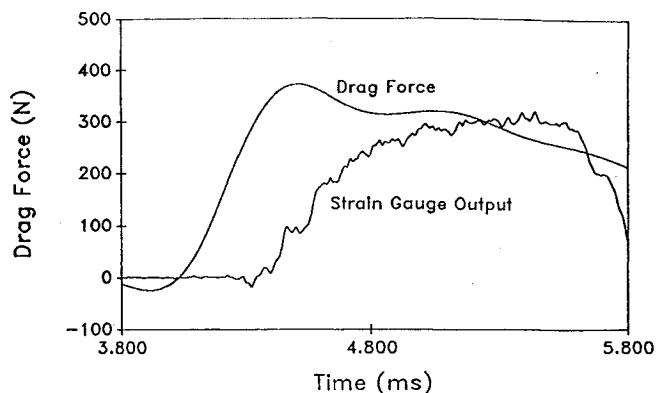


Fig. 1b Comparison between signal from strain gauge bridge before (strain gauge output) and after (drag force) deconvolution for a bluntness ratio of 0.216, nose radius of 10.8 mm.

Received March 7, 1994; revision received April 6, 1994; accepted for publication April 7, 1994. Copyright © 1994 by American Institute of Aeronautics and Astronautics, Inc. All rights reserved.

*Graduate Student, Department of Mechanical Engineering.

†Research Fellow, Department of Mechanical Engineering.

‡QEII Research Fellow, Department of Mechanical Engineering.

§Dean, Faculty of Engineering.

Table 1 Flow properties

Stagnation enthalpy, MJ/kg	Mach number	Static pressure, kPa	Pitot pressure, kPa	Static temperature, K	Flow velocity, km/s	Density, kg/m ³
14.9	5.2	18	580	2000	4.6	0.029

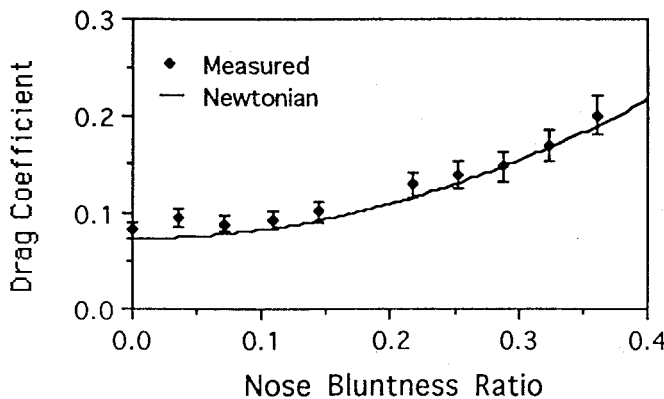


Fig. 2 Drag coefficient vs bluntness ratio from both the measured results and the Newtonian prediction.

constant throughout the test time. The driver gas composition was 90% helium and 10% argon.

The conditions in the test section were numerically determined using ESTC⁵ and NENZF.⁶ The shock speed in the shock tube, the shock tube fill pressure, and the stagnation pressure were measured and used as inputs to ESTC to determine the temperature of the test gas in the stagnation region after shock reflection. The test gas undergoes a steady expansion from the stagnation region to the test flow properties at the exit plane of the nozzle. NENZF is a one-dimensional nonequilibrium code which predicts the properties of the test gas at the exit plane of the nozzle given the stagnation pressure and temperature. Experiments were performed in a test gas of air at a freestream Mach number of 5.2 and a stagnation enthalpy of 14.9 MJ/kg. A summary of the test flow properties is shown in Table 1. This condition corresponds to an equivalent flight speed of approximately 5.5 km/s.

Results and Discussion

The strain gauge signal was deconvoluted numerically as described previously to obtain the time history of the drag on the model. This drag measurement technique is inherently noisy as the deconvolution process tends to amplify any noise present in the original output signal $y(t)$. Thus, it was necessary to pass all of the drag measurements resulting from the numerical deconvolution process through a 2-kHz, 6-pole Butterworth low-pass digital filter. Figure 1 shows an example of the measured drag after filtering in comparison with its corresponding strain gauge output signal before deconvolution. An estimate of the accuracy of the technique indicates values are correct to $\pm 10\%$.

The results are summarized in Fig. 2 in a plot of drag coefficient vs nose bluntness ratio. At the smaller nose bluntnesses the effect of nose bluntness on the total drag is small. There is an increase in drag from the sharp nose value of only about 20% at a bluntness ratio of 0.144 (nose radius of 7.2 mm). Beyond this bluntness ratio, however, the drag increases more rapidly so that at a bluntness ratio of 0.36 (nose radius of 18.0 mm) the value of drag is about 145% greater than the drag on the sharp cone.

The Newtonian sine-square law⁷ was used to obtain an approximation of the pressure coefficient on the cone. The Newtonian law modified for blunted bodies⁷ was used to estimate the pressure coefficient over the blunted nose region. The drag coefficient was calculated based on these approximations and is also plotted in Fig. 2. There is good agreement between the measured drag coefficients and the Newtonian predictions. This would indicate the absence of any real gas effects on blunted cone drag in this hypervelocity flow. This is in agreement with blunted cone studies made in a hypervelocity ballistic range.³

Conclusions

The results indicate that, for small cone angles, the drag of a blunt cone in a hypervelocity flow is reasonably well predicted by the Newtonian sine-square law modified for blunt bodies. This suggests the absence of any real gas effects on the total drag on a blunted slender cone in hypervelocity flow.

The effect of nose bluntness at the smaller bluntness ratios is relatively small, with about a 20% increase in drag at a bluntness ratio of 0.144. This is encouraging for the design of a hypervelocity space plane or a centerbody for an axisymmetric scramjet where a slightly blunted nose is required to reduce stagnation point heating. Beyond a bluntness ratio of 0.144 the drag increases more rapidly with bluntness.

Acknowledgments

The authors are grateful for the support received from the Australian Research Council under grant AE9032029 and the ARC Queen Elizabeth II Fellowship Scheme (for D. J. Mee).

References

- Stalker, R. J., and Morgan, R. G., "The University of Queensland Free Piston Shock Tunnel T4—Initial Operation and Preliminary Calibration," NASA CR-181721, Sept. 1988.
- Sanderson, S. R., and Simmons, J. M., "Drag Balance for Hypervelocity Impulse Facilities," *AIAA Journal*, Vol. 29, No. 12, 1991, pp. 2185–2191.
- Welsh, C. J., Lawrence, W. R., and Watt, R. M., "Real Gas Effects on the Aerodynamics of Blunt Cones as Measured in a Hypervelocity Range," AIAA Paper 80-0373, Jan. 1980.
- Sanderson, S. R., Simmons, J. M., and Tuttle, S. L., "A Drag Measurement Technique for Free Piston Shock Tunnels," AIAA Paper 91-0549, Jan. 1991.
- McIntosh, M. K., "Computer Program for the Numerical Calculation of Frozen and Equilibrium Conditions in Shock Tunnels," Dept. of Physics, Australian National University, Canberra, Australia, 1968.
- Lordi, J. A., Mates, R. E., and Moselle, J. R., "Computer Program for Numerical Solution of Nonequilibrium Expansion of Reacting Gas Mixtures," NASA CR-472, 1966.
- Anderson, J. D., *Hypersonic and High Temperature Gas Dynamics*, McGraw-Hill, New York, 1989, pp. 46–56.

Enhanced Mixing of Multiple Supersonic Rectangular Jets by Synchronized Screech

R. Taghavi*

University of Kansas, Lawrence, Kansas 66045
and

G. Raman†

NYMA, Inc., Brook Park, Ohio 44142

Introduction

THERE have been several investigations of screech tones in underexpanded jets. It was shown by Glass¹ and Krothapalli et al.²

Received April 16, 1994; revision received June 3, 1994; accepted for publication June 11, 1994; presented as Paper 94-2325 at the AIAA 25th Fluid Dynamics Conference, Colorado Springs, CO, June 20–23, 1994. Copyright © 1994 by the American Institute of Aeronautics and Astronautics, Inc. All rights reserved.

*Assistant Professor, Department of Aerospace Engineering. Senior Member AIAA.

†Senior Research Engineer, NASA Lewis Research Center Group, Experimental Fluid Dynamics Section, Cleveland, OH 44135. Member AIAA.